

Urban canyon geometry: how variations influence sky view factor, air and surface temperature.

Heidi Noelle Zutter

Abstract

An urban canyon is a basic urban surface unit comprised of the walls of adjacent buildings, the ground (street) between, and the air volume enclosed within. It is important because of its potential to explain the urban heat island. Because of its geometry, an urban canyon can trap solar radiation and increase the heat of the urban area in comparison to the surrounding rural countryside. Understanding this geometry and its consequences can aid urban street design and energy conservation.

Previous studies have shown that urban canyon geometry such as height-to-width (H:W) relationships, sky view factor (SVF), orientation, and building materials can influence the surface and air temperatures found within the canyon. However, these studies have primarily investigated only one particular urban canyon geometry and so little has been done to intercompare urban canyons. The objectives of this study therefore were (1) to measure SVF of urban canyons of differing orientation, using a number of different methods, and compare the results, (2) to apply SVF results to air and surface temperatures and see how they varied between canyons and (3) to apply a particular SVF method to a mobile transect of SVF and see how SVF changes along a route.

SVF results varied depending upon the method used to measure it. The method that was deemed as most accurate was the automated analysis of Nikon imagery. Using this method, the mobile transect appears to be a valuable method to see how SVF varies along a particular route. SVF (from automated analysis of Nikon fisheye imagery) and air temperatures and surface temperatures appear to be linearly related, but when canyon orientations are accounted for, this relationship loses significance. The size of the sample (only 10 canyons) may not be adequate to determine the significance of the relationship completely. When SVF (from H:W) is compared to air temperatures, the results are such that air temperature and SVF are not linearly related, which may explain the contradiction in what the results indicate (using automated analysis of Nikon fisheye imagery) vs. the results from previous studies (using SVF from H:W). Further study is necessary, with a larger sample size.

1. Introduction

An urban area is comprised of many buildings that when in close proximity to each other form a basic urban surface unit called an urban canyon. The urban canyon is thus a

fundamental unit comprising the urban canopy layer, which is defined as the layer of air from ground to roof-level in an urban area. Urban canyons vary in geometry based on the heights, lengths, and spacing of the buildings that define them. The geometric relationships within them can influence the absorption and emission of incoming solar and outgoing longwave radiation within the urban area and can have a significant impact on the energy balance and temperature of an urban area.

1.1 Statement of the problem

An urban canyon is comprised of the walls and ground (road, garden, etc.) between two adjacent buildings as well as the canyon-air volume, which has three sides with active surfaces (walls and ground) and three open sides (ends and top) (Oke 1987). Studying urban canyons and their respective geometry is worthwhile because of their potential in explaining the urban heat island. An urban heat island occurs when the air in an urban area (city) is warmer than that of the surrounding rural (countryside) area. According to Oke (1987), the air becomes warmer in the urban area because urban geometry and density of development influence processes such as the trapping of incoming solar and outgoing long-wave radiation. Thus, knowledge of canyon climate with respect to canyon geometry and the influence of meteorology help to aid urban street design.

While much research has been done on the climate and effects of a single urban canyon, little to no work has been done to compare different canyon geometry and their effects on variables such as sky view factor (SVF) and temperature (of air and surfaces). The objective of this study, then, was to intercompare canyon geometry (size, orientation/direction) and SVF to see how it impacts air and surface temperatures.

Additionally, H:W relationships have traditionally been used to estimate SVF. A number of other alternative methods are evaluated in this study.

1.2 Background

Studies into urban canyon geometry (canyon orientation and SVF) and its effects on radiation fluxes, and air and surface temperature differences have thus far concerned themselves primarily with only one particular type of urban canyon geometry. However, when these studies are looked at together we begin to see the changes that different height-to-width (H:W) ratios, SVFs, and orientation of canyons can have.

1.2.1 Sky View Factor (SVF)

Sky view factor is the fraction of overlying hemisphere occupied by sky. For example, a SVF of one would be for an open site such as a wide field or the top of a tall building where there are no obstructions blocking a portion of the sky from view (Figure 1a). In urban areas, buildings and vegetation decrease the fraction of sky visible from the ground (Figure 1b). Urban geometry, which is then related to SVF, thus has implications in blocking some of the direct beam of radiation from the sun. According to Oke (1987), urban geometry influences the trapping of incoming solar and outgoing longwave radiation. This allows the urban air to become warmer. By day, a canyon is especially good at absorbing heat because its geometry acts to trap reflected solar radiation and its materials are often good heat stores. At night, the loss of heat from within canyons is slowed by the screening of the sky energy sink by the bordering of buildings (Arnfield 1982).

Mills and Arnfield (1993) found that, as street canyons become increasingly narrow, they become increasingly isolated in terms of heat exchange with the atmosphere above.

Additionally, Arnfield and Grimmond (1998), using a north-south canyon orientation in a model, found that a larger fraction of available canyon net radiation is stored when wall height is large in relation to floor width. Essentially, the narrower a canyon becomes the less radiation that is emitted back out into space because of trapping and so a larger fraction of the net canyon radiation is stored.

Eliasson (1996) found surface temperature to be statistically correlated to SVF. Sky view factor thus has a potential influence on the surface temperatures of urban canyons. Sakikabara (1996) compared canyons of H:W ratios of 0.71 and 2.04 respectively and found no surface temperature difference between the roofs. However, the surface temperature at the center of the canyon with the H:W ratio of 0.71 was generally higher than that when the H:W ratio was 2.04. The difference of maximum heat release between them exceeded 50 Wm^{-2} .

Sakakibara (1996) also compared the surface temperature at the center of the urban canyon street floor with that in a parking lot model (open site) (SVF=1). He found that the urban canyon street floor cools more slowly than that of the parking lot due to the effect of urban geometry. During the daytime, the urban canyon absorbs more energy than the parking lot and the amount of heat released in the urban canyon is twice as much as that of the parking lot at night.

Air temperature could not be statistically correlated to SVF by Eliasson (1996). Differences in air temperatures between open areas and canyons were close to zero for all SVFs, except for SVF=1. Differences in air temperature between areas with SVF=0.9 and SVF=1.0 could be explained by different size and surface material.

1.2.2 Canyon orientation

A canyon's orientation can influence radiation received and trapped as well as surface and air temperature differences. Oke and Nunez (1977) investigated an urban canyon of north-south (N-S) orientation. They found that the canyon orientation impacted the energy balance. Maximum irradiance of the canyon floor was near solar noon. However, maximum irradiance took place 1.5 hours before solar noon on the east wall and 1.5 hours after solar noon on the west wall. They also found that the floor of the N-S canyon was, in absolute energy terms, the most important exchange surface in the energy system.

In 1988, Oke and Nakamura reported an investigation of an urban canyon oriented in the east-west (E-W) direction. They discovered that because of its orientation, and the latitude (Northern Hemisphere), only the north (equator-facing) wall and a portion of the canyon floor received significant quantities of direct beam solar radiation for most of the days. They also found large surface-air temperature differences. On the north wall, which received direct solar irradiation during the day, the surface was always warmer than the air.

Sakakibara (1996) investigated an E-W oriented canyon. He found that the canyon wall of the north building and the street floor absorbs more heat during the daytime hours, while the canyon wall of the south building absorbs more in the morning. Heat release from the north canyon wall is at a maximum just after sunset.

Sakakibara found the surface temperature of the canyon street was highest of the urban surfaces during the day, while the maximum temperature of the south building wall was the lowest of the canyon surfaces and its time of occurrences lagged behind other surfaces. However, this may have been due to differences in building materials.

Sakakibara tested this in his model and found that the surface temperature of the asphalt roof was higher than that on the concrete roof and floor, and in general the surface temperature on the roof was higher than that on the floor, despite both being composed of the same materials.

1.2.3 Building materials

Little is known of the influence of building materials on radiation, surface, and air temperature. Arnfield (1990) found that material differences between the walls and the floors of the canyon and heated building interiors enhanced differences among the cooling rates exhibited by different canyon geometry. Additionally, Sakakibara (1996) found that the surface temperature of an asphalt roof was higher than the surface temperature of a concrete roof or floor. This would not be surprising, since asphalt is much darker in color than concrete and so is probably much better at absorbing heat.

2. Methodology

The study site was confined to the urban areas of downtown and a southwest portion of the Indiana University campus in Bloomington, Indiana (Figure 2). Ten urban canyon locations (Figure 2) were selected within this area from within which measurements of SVF, canyon geometry, air temperature, and surface temperature were taken. Five of these canyons are oriented N-S, and five are oriented E-W. The study took place from March 1999 through August 1999. The air temperature data and a first set of fisheye photographs along with measurements of canyon geometry (to determine SVF) were taken before leaf-out (fisheyes on April 7, 1999 and air temperature from March 30, 1999 until April 16, 1999). Surface temperature data were taken as the leaves had just started to come out (April 13, 1999). LAI 2000 data (also to determine SVF) also were taken

just prior to the leaf-out (April 4, 1999). The second set of fisheye photographs was taken in the summer, under full-leaf conditions (June 26, 1999) and the mobile transect SVFs also were taken during full-leaf (August 1, 1999).

2.1 Observations of sky view factor

Sky view factors for each of the canyon sites were determined in a number of ways through canyon geometry (H:W measurements), fisheye photos (manual and digital cameras with fisheye lenses), and the Li-Cor LAI 2000 instrument.

2.1.1 Height-to-width (H:W) relationships

One way of determining SVF is through the use of H:W relationships, which provide basic data on the geometry of the urban canyon. These H:W ratios are determined from measured clinometer (Suinto Co., PM-5/360 PC) angles and measured canyon dimensions (using a measuring tape).

The clinometer was used to measure the angle from the eye-height of the operator to the top of each wall of the canyon. The operator stands in the center of the canyon and takes an angle measurement for each wall. The operator's distance from each wall as well as the operator's eye-level height are then measured with the tape measure. Using the distance of the operator from each wall of the canyon, and the angle as determined from operator eye-level height to the top of each wall, the height of the building above the person's eye-level could be determined. To get the total height of each canyon wall, the eyelevel height of the operator was added on to the height of the above eye-level calculation. From this data, then, the height and width of the canyons can be determined from geometric relationships and a H:W ratio can be assigned to each canyon.

2.1.1.1 Calculation of SVF (manual analysis)

Each of the canyons was asymmetrical, with walls of differing heights, so the formula $SVF = \cos(\tan^{-1}(2H/W))$ (Oke 1987) was used. This formula was used once for each wall and the results were then averaged to get a mean SVF for the entire canyon. Table 1 was created to show the clinometer angles and measured dimensions of each canyon, including the average H:W ratio and average SVF as determined from the formula from Oke (1987).

The height at which SVF is measured from will influence the final SVF result, because as the height is increased (or decreased), the amount of sky that can be seen is also increased (or decreased). Consequently, since SVFs were measured at a variety of heights depending upon the method (camera height=1.27 m, LAI height=2.21 m, and ground (for H:W)) the H:W ratios were recalculated later, for camera and LAI height, for intercomparison purposes.

2.1.2 Fisheye photographs

Fisheye photographs were taken using a camera and a fisheye lens mounted on a tripod in, approximately, the center of each canyon. Two different cameras and fisheye lenses were used.

In accordance with previous studies (Clark and Follin, 1988), hemispheric photographs were taken using a vertically mounted SLR camera (Olympus OM-1 35 mm) equipped with a Sigma F4 fisheye lens. The Sigma lens has a field of view of 160° (Clark and Follin, 1988). To collect the images for analysis, the camera was mounted on a tripod at a height of 1 m, leveled horizontally using a bubble level, and always oriented so that north corresponded to the top of the photograph. Color film (200 ASA) was used.

In most instances, an F-stop of 5.6 was used, although it and the shutter speed were adjusted based on readings from a light meter.

Using this camera and lens, the first set of fisheye photographs was taken on April 7, 1999, at 1705 under clear, sunny conditions. Ideally these photographs are also taken on overcast days, since bright sunlight can obscure objects in the pictures. However, because it was evening, the sun was not visible in most of the photographs, or if it was it affected the pictures only slightly.

The Nikon Coolpix 950 digital camera and compatible Nikon FC-E8 fisheye converter lens were used to take hemispheric fisheye photographs as well. The FC-E8 lens has a field of view of 183 degrees. The Nikon camera was vertically mounted to a tripod at a height of 1 meter and leveled using a torpedo level placed across the top of the lens cap. A torpedo level was used rather than a bubble level (for example) since the lens cap was not flat and so the torpedo level could span the diameter of the cap and thus give an accurate level indication.

On June 26, 1999, using this camera and fisheye lens, a second set of fisheye photos for all canyons (except for NS 1.27 and NS 1.50) were taken. The digital output of the photos taken with this camera is a much higher resolution than the scanning resolution of the other photos, and so accuracy should thus be improved. The NS 1.27 and NS 1.50 canyon sites could not be reanalyzed because of construction that was taking place within the canyons themselves at the time.

The fisheye photos from both types of cameras were then analyzed for SVF in two different ways, using a manual and automated method. These methods are now described in detail.

2.1.2.1 Polar coordinate method (manual analysis)

The polar coordinate method involved taking the developed fisheye photographs from the manual SLR 35mm camera or digital Nikon fisheye photographs and enlarging them to fit polar coordinate graph paper. The photographs and polar coordinate paper were copied onto transparency film and laid on top of one another (Figure 3). The relative amounts of vegetation and building were added up (counting number of squares of each) and entered into a spreadsheet, which calculated the SVF (using an area weighted Johnson and Watson (1984) method).

2.1.2.2 Digital program (automated analysis)

For the photos taken with the Sigma OM-1 camera and fisheye lens, photo film rolls were developed and then the resulting pictures were scanned into digital format using a Plustek OpticPro 4831P scanner. The photos were cropped to be square pixels and then saved in GIF format using Micrografx Photo Magic (version 4.0a). These photos were then brought into a program called XV 3.10a, by John Bradley, and then saved as XPM (grayscale) format which converted them to black and white.

The photos taken with the Nikon Coolpix camera and fisheye lens were already in digital format to begin with, and so the pictures were downloaded from the camera directly to the computer. They were in JPG format initially. These photos were brought into Paintshop Pro, version 5.0 and cropped to be square (750 square pixels). These photos were then formatted to a contrast of 100% (black and white) and saved as PGM (grayscale) format. Figure 4 shows an example of the editing performed on these photos prior to the digital analysis.

The XPM or PGM files were then analyzed using a FORTRAN 90 program written by Dr. Sue Grimmond (SVF.exe). This program takes the XPM or PGM files and converts them to polar coordinates with 70 concentric rings, using the method of Johnson and Watson (1984) to weigh each concentric ring to determine the SVF.

2.1.3 LAI 2000

The LAI 2000 plant canopy analyzer (Li-Cor Inc., Lincoln, NE) was used as an alternative method to quantify SVFs. The LAI 2000 gathers data on vegetation-area index—or the amount of vegetation area that is present. It detects the penetrating diffuse light at five angles (0-12°, 15-28°, 31-43°, 45-58°, and 61-74°) simultaneously (Li-Cor, 1992) and yields a value that indicates the fraction of the sky that is not blocked by foliage. This value ranges from 0 (no sky visible) to 1 (no foliage visible). Full details on the theory of operation of the instrument are presented by Welles and Norman (1991). The response time of the instrument is milli-seconds.

The inverse of this index is the DIFN, which quantifies the amount of sky (rather than vegetation) that can be seen. The DIFN is used here to see how it compares with the SVFs determined by other methods. There are several problems with using this instrument to determine SVF. One is that the LAI 2000 calculates DIFN by measuring radiation and, thus, any radiation reflected off the sides of buildings would result in errors. The instrument only senses radiation at wavelengths $< 490 \mu\text{m}$ so, provided the buildings are not strongly reflective, over-estimations likely will be small. A second problem is, that the LAI 2000 has a full field of view of 148°, which is much less than the full 180° needed for proper SVF analysis.

The LAI 2000 is ideally suited for overcast conditions since the bright sun can interfere with the accuracy of the readings. Although, there is some ability to account for other sky conditions when analyzing the data. The LAI 2000 comes with a set of caps for the sensors of the instrument, which are designed to block undesired objects (i.e. people, the sun, etc) from the sensor's view.

The LAI data set was collected at 0730 on Sunday April 4, 1999, on a bright, sunny, and clear day. Although the LAI 2000 is ideally suited for overcast conditions, because the appropriate weather was not available the measurements were made early in the morning, just after sunrise, before the sun rose high in the sky. A quarter cap was placed on the instruments facing the east direction (direction of rising sun) in the hope that it would block out most of the direct sunlight.

To obtain the DIFN values from within the urban canyons, two LAI 2000 sensors were used. One of the sensors was placed in an unobstructed location throughout the measurement period and the second sensor was taken to each of the individual canyons for measurements. Initially both were taken to the open site and were calibrated while mounted on tripods at approximately 1 m height. Then, one (the "upper" sensor) was left mounted at the open site (on top of a parking garage) for continuous measurements, which were recorded every 15 seconds. The lower sensor was taken (without tripod) to each individual canyon site and 10 measurements were taken at each site. Multiple measurements were taken to account for errors in keeping the sensor level (each sensor is equipped with a bubble level) while taking measurements. The LAI measurements were taken at approximately 2 m height in the canyons.

2.1.3.1 DIFN calculation (automated analysis of LAI2000)

The LAI 2000 dataloggers were downloaded and then the continuous data from the open site and the fixed measurement data from the ten canyon locations were matched and merged according to the LAI procedures manual (LiCor, 1992). The DIFN results from analysis of the merged data using LAI 2000 accompanying software (LiCor, 1992) were then taken as the SVF for each canyon. The DIFN results for each canyon were then compared with the automated analysis of the Sigma lens imagery to the reference SVF results.

2.2 Applications using canyon geometry and sky view factor

Measurements of air temperature and surface temperature were also made and compared with the canyon geometry, using SVFs. Additionally, continuous measurements of SVF were made along a route and analyzed for accuracy and feasibility of investigating how SVF varies for a larger area (mobile transect).

2.2.1 Surface Temperature

In order to see if heat energy radiating off the buildings and ground impacts the temperature of the air within the canyon itself, an *Omega* Infrared Thermometer (Model 0S71) was used to measure the surface temperature of the canyon walls and floor. The emissivity on the instrument was kept constant at 0.99, since most of the wall and floor surfaces were concrete, brick, and stone. This value was chosen mainly out of convenience to avoid determining exact emissivities of particular surface types and adjusting the instrument to them accordingly at each canyon site. The surfaces were all dark in color and so would absorb more heat from the sun, than surfaces of lighter color materials such as wood. Upon additional thought, the emissivity probably should have

been adjusted to around 0.90 at the most if a specific emissivity were to be chosen and kept constant. An emissivity of 0.90 (or even less) would be more realistic given the variety of surfaces and the fact that none of the surfaces were black (or true blackbodies), where a true blackbody would have an emissivity of 1.00. If this study were just on building materials and surface temperature, the exact emissivities of the surfaces would have been used to achieve greater accuracy. A larger sample would also have been used.

Measurements were taken on April 13, 1999 between 1830 and 2000 as the sun was setting on a clear and sunny day. The measurements were taken at regular heights in a line down the center of the respective canyon walls, and across the canyon floor, at 0.25 intervals of the wall height as shown in Figure 5. From these surface temperature measurements and assumed emissivity of surfaces (0.99), the radiation emitted was calculated using Stefan-Boltzmann's law.

Surface temperature measurements at the approximate canyon intervals shown in Figure 5 are shown in Table 2, along with building materials of each surface (ground, wall1 and wall 2). Mean surface temperatures for each surface (walls and ground) were calculated and then averaged for a mean surface temperature in each canyon and these results are shown in Table 2. The mean surface temperature of each urban canyon calculated was entered into the Stefan-Boatman law: $E = \epsilon \sigma T^4$, (where $\sigma = 5.67032 \times 10^{-8}$ W m⁻² K⁻⁴ is constant and ϵ is the emissivity (0.99)) in order to determine the radiative energy given off in each canyon (Table 3).

2.2.2 Air temperature

In order to investigate how canyon geometry influences air temperature, it was necessary to document the air temperature within the canyons over a certain period of

time. *Onset* HOBO stowaway XTI datalogger sensors were mounted at each location to gather air temperature data within the canyons. Hobo sensor air temperature data were used, in addition to the Bloomington weather station air temperature data, to see how the air temperature within the canyons differed from the air temperature of an open site, and to see if surface temperatures of the canyon surfaces influenced the air temperature of the canyons. Air temperature data were compared between canyons as well to determine if orientation had any influence.

The temperature range of the HOBO sensors is - 5 °C to + 37°C. Information on accuracy and resolution can be seen in the appendix. The sensors were programmed with compatible *Logbook* software to sample data every 60 seconds and record averages every 15 minutes, for 18 days. Data collection began on March 30, 1999. The sensors were mounted at fixed locations in the center of the canyons at a height of about 5 m. Each HOBO sensor was placed in a radiation shield. Temperature data from the Bloomington weather station, that is located in a relatively open grass field at the northernmost part of the Indiana University campus, served as the open reference. An *Onset* HOBO sensor was placed at this site as well for data comparison with temperature data at the canyons sites. On April 16, 1999, the sensors were removed and the data was downloaded into text files for comparison. For an unknown reason, the data from the open site was not on the Hobo sensor when it was downloaded. Consequently data from the Bloomington weather station (National Weather Service, 1999) were used for all data analysis involving the open site.

To account for inter-instrument differences, the Hobo sensors used were also used to generate data for intercomparison. The 11 sensors available were placed in the same

location outside for about half an hour and collected air temperature data over this period. The data were downloaded from each sensor into text files. The intercomparison files were looked at as a time-series and the maximum and minimum temperatures were examined for maximum instrument differences. The maximum temperature difference between instruments for the maximum temperature on the time series was 2.75 degrees Celsius, and the maximum temperature difference between instruments for the minimum temperature on the time series was 0.38 degrees Celsius. Thus, 2.75 degrees Celsius is the temperature used for the maximum inter-instrument differences. This difference is shown as error bars on all air temperature comparison graphs. The inter-instrument differences should, however, be much lower than 2.75 degrees Celsius in most instances.

2.2.3 Mobile transect

Part of this study involved mapping SVF for the more general areas around the 10 study canyons. On Sunday, August 1, 1999, using the Nikon Coolpix 950 digital camera and fisheye lens converter, a route was driven starting from the corner of Kirkwood and Walnut and ending up in a circle drive behind the student building of Indiana University (Figure 6). The field vehicle was a passenger car equipped with a sunroof. The sunroof, when open, allowed the passenger to hold the camera and take pictures as the driver drove the car approximately down the center of the road. A torpedo level was attached to the bottom of the camera with rubber bands to secure it in place so that while the car was in motion, the camera could be held approximately level as each picture was taken. Driving at about 10-15 mph pictures were taken at semi-regular intervals, several times in each block and intersection. A total of 160 pictures were taken on this route and

downloaded for analysis. An example of these photos, taken from three portions of the transect, are shown in Figure 6.

The digital photos from the mobile transect were cropped and formatted in Paintshop Pro 5.0 for analysis with the program SVF.exe. The photos were then analyzed visually to determine which of the photos originated from each intersection along the route. Then, the photos between each intersection were assumed to have been evenly spaced. To chart the change in SVF along the transect the distance of each photo was measured in mm from the start of the transit on a Bloomington map. The distances (from the start) of each intersection were first determined and then the distances between intersections were divided by the number of pictures between each intersection to find the distances of each of the pictures between intersections. These distances in mm measured on this map were then converted to meters in reality. These were then the distances used to plot the change in SVF with distance from the start of the transect.

3. Results and Discussion

Now the results will be looked at in further detail and discussed.

3.1 Sky view factor: a comparison of methods

In this study, SVF was determined using four methods: H:W measurements, manual analysis (polar coordinate graph paper and counting squares), automated analysis (digital program--SVF.exe) and LAI 2000. The results obtained using each of these methods varied. All canyons referred to in the discussion to follow are named according to their orientation and their average H:W ratio (e.g. NS 1.40).

Figures 7, 8, 9 and 10 were generated to compare the SVF methods used. The results from the automated analysis of the Nikon digital photos with SVF.exe were used as the

reference. Figure 7 compares the SVF calculated from H:W ratios--calculated at ground height, camera height, and LAI height.

Figure 7 compares the SVF determined from H:W ratio measurements at several different heights with the SVF determined through automated analysis (SVF.exe) of Nikon digital imagery. H:W measurements were determined for the ground level initially. SVF was then determined from these original measurements of H:W at ground level and also determined for the H:W measurements calculated for the heights that the camera (height = 1.27 m) and LAI measurements (height = 2.21 m) were taken at. As can be seen in Figure 7, SVF varies depending on the height of the measurements within the canyon. The SVF from H:W measurements at all three heights vary from the reference of the automated analysis of Nikon fisheye imagery.

Figure 8 compares the SVF determined from the manual polar coordinate analysis of color JPG and black and white PGM printouts of the digital Nikon imagery with the SVF determined from the automated Nikon analysis. The PGM imagery differs from the JPG imagery because it has been converted to black and white and in the process has been edited to counteract washout of buildings and vegetation. The results show, however, that the difference in SVF calculated is very minor due to image editing. The automated analysis is probably more reliable than the manual analysis (by counting) since there is human subjectivity when accumulating partial areas on polar coordinate graph paper.

Figure 9 shows a comparison of the manual polar coordinate analysis of the original Sigma lens photographic print with the automated analysis of the Nikon images. Many problems were encountered when the Sigma lens photographic prints were processed

(e.g. improper printing, etc). This led to problems centering the photograph correctly for the manual analysis by polar coordinate graph paper. Thus, the results from the manual analysis of the Sigma lens prints vary from the Nikon automated analysis.

Figure 10 compares the results of the automated analysis of Sigma lens scanned imagery and of LAI 2000 data with the automated analysis of the Nikon images. LAI 2000 (DIFN) yields consistently higher results. This may be explained by the potential for overestimation due to significant reflectance off building materials, since the LAI 2000 can sense wavelengths of less than 490 micrometers. Digital analysis of the Sigma lens imagery again varies from that of the Nikon imagery due to errors in photo processing and scanning.

No method used is without error or disadvantages. The LAI 2000 provides an easy method to collect mobile data, both in terms of data collection and storage. Post field data calculation is rapid and there is some limited ability to adjust processing based on sky conditions. However, the LAI 2000 has more restricted sky conditions under which it performs accurately; ideal conditions are overcast skies. The manual camera with Sigma fisheye lens has the disadvantage of having to wait for film to be processed (of varying quality). Additionally, print accuracy and scanning can be highly subjective, especially when a lot of vegetation is present. This method requires a test set of images to be created to ensure accuracy and consistency of the method when different operators are in charge. The digital camera (Nikon Coolpix) has the advantage of being able to perform image corrections more accurately before calculating SVF (to counteract building and vegetation washout due to solar glint). Also, the imagery from all the sites is then available for other analyses.

The SVFs from the H:W relationships are quite different from those calculated by the polar coordinate method. Though there was some error involved, the polar coordinate method (manual (counting) or automated (program)) provides a much more accurate method of calculating SVF because it accounts for vegetation in its calculation (unlike H:W method) and because it introduces the least amount of human error (no tape measure or clinometer). Vegetation has the effect of shading the canyon floor and walls, allowing less radiation to be absorbed, thus keeping the canyon cooler. Many previous studies used H:W ratios as SVFs (Eliasson 1996, for example). This may work for modeling where other factors such as vegetation and symmetry can be eliminated or controlled for, but when investigating actual canyons, there are factors such as vegetation and other objects that can block sky view. Because several of the canyons included vegetation, the polar coordinate method (manual or automated, but especially the automated analysis) served this study best for making comparisons.

3.2 Surface temperature

To compare potential SVF (automated Nikon analysis) influence on surface temperatures, Figure 11 was created to compare SVF versus surface temperature for all the canyons. Figures 12 and 13 were created to compare this for north-south and east-west canyons, respectively, to eliminate the factor of canyon orientation on the comparison. For the canyons NS 1.27 and NS 1.50, the manual analysis of the Sigma imagery was used since Nikon imagery was not available (not taken). On these graphs a linear regression line was fitted to the data and the regression equation and R-square value are shown.

Figure 11 shows the mean surface temperature related to SVF (automated analysis) for all the canyons. The R-square value of 0.3202 suggests that SVF has minimal influence on the mean surface temperature of the canyons. Figure 12 and 13 look at SVF compared to the mean surface temperature, accounting for north-south and east west canyon orientation, respectively. In Figure 12, for the north-south oriented canyons, the R-square value of 0.0764 (which is very small) suggests that SVF has little influence on the mean surface temperature of these canyons. In Figure 13, for the east-west oriented canyons, however, the R-square value of 0.5524, suggests that the SVF may influence the mean surface temperature of these urban canyons. The fact that the relationship is less significant for north-south canyons is not obvious. Overall, the slope of the line indicates that as SVF becomes larger, the mean surface temperatures decrease. This would seem to make sense, because with a greater SVF that means that there is less geometry available to trap radiant heat energy. Thus, the canyon surfaces could emit more energy and thus have lower surface temperatures. The sample size available for this analysis is very small (too small), and would need to be increased to examine this relationship more closely. Eliasson (1996) found surface temperature to be statistically correlated to SVF, although SVFs from H:W relationships were used rather than SVFs from digital fisheye imagery. Further investigation is thus necessary.

3.3 Air temperature

To compare canyons and their respective air temperatures, Figure 14 was created to show a plot of air temperature readings for March 30, 1999 (clear conditions) and Figure 15 was created to show a plot of air temperature for April 1, 1999 (cloudy conditions). Figure 16 shows Bloomington weather station (open site) air temperature data as a time

series for March 30, 1999, through April 1, 1999. To compare canyon orientation and air temperature, Figures 17 and 18 were created displaying the trends for the north-south and east-west oriented canyons.

In addition, air temperature differences compared to SVF between the canyon sites was looked at (Figure 19). The canyons oriented north-south and east-west were then looked at separately (Figures 20 and 21), since orientation may impact air temperature differences between the canyons.

Sky view factors (calculated using the H:W ratios) were then used to compare how they related to air temperature in north-south and east-west canyons in Figures 22 and 23. These results were compared to those from Figures 20 and 21. In each of the graphs, a linear regression line was fit to the data and an R-square value and regression equation are both shown.

3.3.1 Relationship with SVF

Figure 19 shows the relationship between canyon SVF (automated analysis Nikon) and air temperature, with an R-square value of 0.3333. This suggests that SVF does influence the air temperature of the canyons in the same way as it appeared to influence the mean surface temperature of the canyons (i.e. as the SVF increases, the air temperature decreases due to less geometry available to trap heat energy). In Figure 20, for the north-south oriented canyons only, the relation between SVF and air temperature has an R-square value of 0.0148, suggesting that SVF is not related to the air temperature of these canyons. However, in Figure 21 for east-west oriented canyons, the relationship has an R-square of 0.5949 for SVF and air temperature. From these figures, it appears that SVF does influence the air temperature of the east-west oriented urban canyons but

not of the north-south oriented canyons. This would partially contradict Eliasson's (1996) finding that air temperature was not statistically correlated with SVF. One difference might be that Eliasson (1996) used H:W ratios for SVF, whereas this study used the automated analysis (with Nikon imagery) of SVF that accounts for vegetation in the analysis. However, this would not explain why the north-south oriented canyon SVFs were not correlated to air temperature. An explanation for this result might be that the north-south canyons only receive direct sunlight rays for a few hours when the sun is directly overhead at midday. The east-west oriented canyons, however, are exposed to direct rays from early in the morning until late in the afternoon. Thus, orientation may be a factor. However, this may be again due to the size of the sample being so small. Further investigation using a larger sample is necessary for conclusive results.

Figures 22 and 23 show the SVF calculated from H:W ratios plotted against air temperature for north-south and east-west oriented canyons to investigate this further. It is clear that in comparing the SVF calculated from H:W relationships to air temperature, the relationship between them becomes much less obvious. Using SVF from H:W ratios, the R-square values decreased to 0.0059 for the north-south canyons and to 0.554 for the east-west canyons. However, the east-west canyon SVF can still be considered correlated to air temperature, although to a lesser extent with H:W than with SVF from the automated analysis of Nikon digital imagery. This is reasonable since the SVF from the Nikon automated analysis accounts for vegetation and should therefore be better at explaining air temperature variations than should SVF from H:W relationships, which only accounts for the geometry of the buildings. This illustrates and possibly explains the reason for contradiction with the results from Eliasson (1996).

3.3.2 Relationship with canyon orientations

Air temperatures for all 10 canyons over a day's time are shown in Figure 14 for March 30, 1999 (day 89) that was a clear day and also in Figure 15 for April 1, 1999 (day 91), which was a cloudy day. In both figures, one can see that the five canyons in the east-west orientation heated up faster (on average) in the morning than the five canyons oriented in the north-south direction, and of course stayed warmer the longest in the evening due to the additional heat they had during the day. This is of course excluding inter-instrument differences (error bars) because this would be terribly difficult to look at on these figures. These results make sense since the east-west oriented canyons are exposed to the sun's radiant beams all day while the north-south canyons are exposed only from late morning to mid-afternoon each day.

Figure 16 shows the air temperature data for the open site (Bloomington weather station), with a SVF of close to one, from March 30, 1999 (day 89) through April 1, 1999 (day 91). Comparing Figure 16 to Figures 14 and 15, it is clear that the open site followed the same general air temperature pattern, but was on average about 5-10 degrees cooler on March 30, 1999 (clear, sunny conditions) and at least 1-3 degrees cooler on April 1, 1999 (cloudy, drizzly conditions). This result makes sense, since urban canyons absorb more heat energy with their materials and also trap solar energy, keeping the temperatures warmer. The open site does not have the geometry to trap heat energy, and also has a lot more vegetation (grass), and so is that much cooler.

Figures 17 and 18 show that the north-south and east-west canyons followed the same general air temperature pattern. The only difference between them appears to be that the north-south oriented canyons have a more sharply defined peak temperature just after

noon. This may be because the north-south canyons are only exposed for a few hours in the afternoon to the sun and so have a short period for maximum temperatures to be reached, whereas the east-west canyons have all day and their peaks are thus more gradual.

3.3.3 Surface temperature influence on air temperature

There is interest in whether or not surface temperature influences the air temperature. In order to examine this, we must look at a pair of canyons without vegetation, with the same SVF and orientation. Materials were assumed to be approximately the same emissivity in all canyons, so this was assumed not to be a factor. *Ceteris paribus*, we assume that the canyons with the higher surface temperatures (energy emitted) would have higher air temperatures as well. In Table 3, canyons “EW 3.14” and “EW 2.88” at the top are both oriented east-west, with approximately the same SVF (0.18 and 0.20) and neither had vegetation within them. The mean surface temperature, and thus mean energy emitted, was highest in the “EW 2.88” canyon, however, the air temperature was highest in the “EW 3.14” canyon. No other canyon pairs were suitable for comparison. From looking at this one instance, one could conclude that surface temperature (heat energy emitted) did not impact the air temperature. However, the sample size is very small and so to draw a firmer conclusion, this obviously needs to be looked at further, with more canyon comparisons and then statistical tests.

3.4 Mobile transect

A look at the mobile method of measuring SVF provides an interesting way to look at how SVF changes across an urban area. Figure 24 shows the results for the mobile transect, change in SVF with distance from the start of the transect (along route), in

downtown Bloomington, IN, through the campus of Indiana University. This Figure has three main areas of particular interest. The first area is from distance 0 meters to about a distance of 1300 meters along the route. This area is representative of downtown Bloomington area, circling the courthouse. This area is relatively open due to wider main streets which are circling the courthouse area of town, which is more open. Thus, the SVFs here are consistently in the range from about 0.68 to about 0.87, which is fairly high for an urban area. The second area of interest is at the distance of about 1400 meters. Here there is a large dive in the SVFs from around 0.90 down to about 0.35, and then back up to 0.90. This is representative of an alley between a 5-level parking garage and another large building. The third area of interest is the area from about 2000 m through to the end. Here the SVF has a much wider range varying from about 0.85 to about 0.27. This area is representative of the campus of Indiana University, which has a marked increase in the number of trees, especially large trees lining the streets and the land to either side of the streets. These trees in addition to many large buildings cause the SVF to drop as low as 0.27.

4. Conclusions

Studies of urban canyons have shown that canyon geometry and materials that make them up can influence the air and surface temperatures of urban canyons. By comparing different canyon geometries and their respective air and surface temperatures, this study went beyond most previous studies that investigated only one particular urban canyon geometry.

Sky view factor varied depending upon the method used to measure it. The method we deemed as most accurate was the automated analysis of Nikon imagery. Using this

method, the mobile transect appears to be a valuable method to see how SVF varies along a particular area (route).

SVF (from automated analysis of Nikon imagery) and air temperatures and surface temperatures appear to be related, but when canyon orientations are accounted for, this relationship loses significance for the north-south canyons. The size of the sample (only 10 canyons) may not be adequate to determine the significance of the relationship completely. When SVF (from H:W) is compared to air temperatures, the results are such that air temperature and SVF are not linearly related, which may explain the contradiction in what our results indicate vs. the results from previous studies. Further study is necessary, with a larger sample size to draw more sound conclusions.

Certainly, urban canyons influence higher temperatures adding to the temperatures experienced within the city. This can be controlled by controlling the sky views of canyons through better planning when constructing buildings and city blocks, especially through the inclusion of vegetation.

Acknowledgements:

To Dr. Sue Grimmond, Janet Nackoney, Justin Schoof, Todd Barnell, and Chad Zutter for their generous contributions of time and effort to this project.

References Cited:

- Arnfield, A.J. (1982) "An approach to the estimation of the surface radiative properties and radiation budgets of cities." *Physical Geography* **3**, 97-122.
- Arnfield, A.J. (1990) "Canyon geometry, the urban fabric and nocturnal cooling: a simulation approach." *Physical Geography* **11**, 209-239.
- Arnfield, A.J. and Grimmond, C.S.B. (1998) "An urban canyon energy budget model and its application to urban storage heat flux modeling." *Energy and Buildings* **27**, 61-68.
- Clark, J.A. and Follin, G.M. 1988. A simple equal area calibration for fish-eye photography. *Agricultural and Forest Meteorology* **44**, 19-25.
- Eliasson, I. (1996) "Urban nocturnal temperatures, street geometry and land use." *Atmospheric Environment* **30**, 379-392.
- Johnson, G.T. and Watson, I.D. (1984). "The determination of view factors in urban canyons." *Journal of Climate and Applied Meteorology* **2**, 329-335.
- Li-Cor Inc. 1992. LAI-2000 Plant Canopy Analyzer Operating Manual.
- Mills, G.M. and Arnfield, A.J. (1993) "Simulation of the energy budget of an urban canyon—II. Comparison of model results with measurements." *Atmospheric Environment* **27B**, 171-181.
- Nakamura, Y. and Oke, T.R. (1988) "Wind, temperature, and stability conditions in an east-west oriented urban canyon." *Atmospheric Environment* **22**, 2691-2700.
- National Weather Service (1999) Bloomington, Indiana weather station data from website: <http://tgs7.nws.noaa.gov/weather/current/KBMG.html>.
- Nunez, M. and Oke, T.R. (1977) "The energy balance of an urban canyon." *Journal of Applied Meteorology* **16**, 11-19.
- Oke, T.R. (1987) *Boundary Layer Climates* (2nd ed.), Methuen.
- Sakakibara Y. (1996) "A numerical study of the effect of urban geometry upon the surface energy budget." *Atmospheric Environment* **30**, 487-496.

Welles, J.M. and Norman, J.M. 1991. "An instrument for indirect measurement of canopy architecture." *Ergonomics Journal* **83**, 818-825.

Figures and Tables:

Table 1. Canyon geometry as determined from measured and calculated height, width and sky view factor data

Canyon name	Wall orientation	Measured Width (m)	Clinometer reading (°)	Calculated Height (m)	Average H/W ratio (ground)	Calculated SVF (ground)	Average SVF (ground)
NS 1.40	east	3.61	68.00	6.01	1.40	0.29	0.35
	west	3.61	55.00	4.12		0.40	
EW 3.14	north	3.64	75.00	8.33	3.14	0.21	0.17
	south	3.64	82.00	14.49		0.12	
EW 1.78	north	3.83	70.00	6.80	1.78	0.27	0.27
	south	3.83	70.00	6.80		0.27	
EW 2.88	north	3.87	74.00	8.29	2.88	0.23	0.19
	south	3.87	81.00	13.76		0.14	
EW 1.58	south	5.08	55.65	5.26	1.58	0.43	0.33
	north	5.08	74.65	10.79		0.23	
NS 0.67	east	21.8	57.00	16.14	0.67	0.51	0.57
	west	29.08	48.00	17.69		0.63	
EW 0.88	south	18.93	53.00	14.10	0.88	0.56	0.50
	north	18.93	62.00	19.34		0.44	
NS 1.27	east	9.68	63.00	11.04	1.27	0.40	0.37
	west	9.68	68.00	13.52		0.34	
NS 1.50	east	9.65	70.00	14.79	1.50	0.31	0.32
	west	9.65	69.00	14.11		0.32	
NS 1.00	east	18.6	64.00	20.61	1.00	0.41	0.45
	west	18.6	58.00	16.42		0.49	

Table 2. Infrared surface temperature data from urban canyons, including building materials. For the ground, temperatures 0L to 1.00L indicate temperature readings going from the North to the South (EW canyon) (or vice versa), where L is the length of the ground between the walls. For the building walls, temperatures 0L to 1.00L indicate temperature readings going from bottom to top of wall, where L is the length (or height) of each wall.

Canyon	Material	Surface Temperature (°C)					Mean surface temperature (°C)	Overall mean surface temperature (°C)
		0L	0.25L	0.50L	0.75L	1.00L		
EW 1.78								
ground	pavement	15.44	15.00	14.44	13.44	13.89	14.44	
north wall	brick	15.50	18.50	17.33	13.89	12.61	15.57	14.60
south wall	brick	15.56	16.56	14.39	14.00	8.44	13.79	
EW 2.88								
ground	pavement	18.94	18.78	18.33	17.17	16.56	17.96	
north wall	limestone	16.39	19.56	20.33	20.89	20.11	19.46	19.12
south wall	brick	19.39	20.61	20.44	20.28	19.00	19.94	
EW 3.14								
ground	pavement	15.11	15.06	14.83	14.39	14.89	14.86	
north wall	brick	15.39	19.50	17.39	16.17	15.61	16.81	16.02
south wall	brick	14.72	17.78	17.33	16.78	15.28	16.38	
EW 1.58								
ground	pavement	15.67	15.56	17.94	23.61	23.72	19.30	
north wall	brick	15.94	17.83	17.67	17.72	17.50	17.33	17.83
south wall	brick	22.78	17.06	16.72	14.39	13.39	16.87	
EW 0.88								
ground	pavement	10.00	8.56	16.83	8.11	9.00	10.50	
north wall	limestone	15.83	16.67	16.94	16.67	15.83	16.39	13.49
south wall	brick	12.50	13.78	13.89	13.72	14.00	13.58	
NS 0.67								
ground	pavement	14.17	13.78	12.17	16.22	10.67	13.40	
east wall	limestone	15.39	14.72	16.94	17.61	18.61	16.66	15.48
west wall	limestone	15.56	15.78	17.56	17.17	15.94	16.40	
NS 1.40								
ground	pavement	16.67	16.94	17.33	16.56	16.72	16.84	
east wall	Aluminum siding	17.44	22.44	14.22	14.39	8.00	15.30	16.86
west wall	brick	17.17	19.28	20.22	18.33	17.17	18.43	
NS 1.27								
ground	pavement	12.22	11.72	17.61	11.83	12.83	13.24	
east wall	limestone	15.44	14.83	17.17	16.17	18.83	16.49	14.72
west wall	brick w/ ivy cover	16.33	15.11	13.72	14.06	12.94	14.43	
NS 1.50								
ground	pavement	15.00	13.50	13.39	13.11	12.50	13.50	
east wall	brick	17.00	15.78	16.67	16.61	15.56	16.32	14.97
west wall	limestone	16.28	15.83	15.39	14.28	13.61	15.08	
NS 1.00								
ground	pavement	10.33	12.00	14.61	17.39	13.28	13.52	
east wall	limestone	14.94	14.44	14.00	14.44	16.94	14.96	14.32
west wall	limestone	16.17	14.94	15.22	14.22	11.83	14.48	

Table 3. Canyon intercomparison summary (for 4/13/99, approximately 7:30 pm)

Canyon	SVF (from H:W) ground	Overall mean surface temperature (°C)	Air temperature (°C)	SVF (automated Nikon)	Energy (radiation) emitted (W m ⁻²)
EW 3.14	0.17	16.02	20.06	0.18	391.7
EW 2.88	0.19	19.12	17.47	0.20	408.8
NS 1.40	0.35	16.86	17.45	0.38	396.3
EW 1.58	0.33	17.83	14.96	0.35	401.6
NS 1.27	0.37	14.72	14.75	0.39**	384.7
NS 1.50	0.32	14.97	15.78	0.43**	386.0
EW 1.78	0.27	14.60	18.24	0.44	384.1
NS 1.00	0.45	14.32	NA*	0.29	382.6
EW 0.88	0.5	13.49	15.64	0.52	378.2
NS 0.67	0.57	15.48	15.93	0.54	388.8
open site	1***	NA	13.6	1***	NA
*Hobo sensor stopped working after April 2, 1999--reason unknown					
**Manual analysis of Sigma lens imagery (Nikon not available)					
*** SVF of 1 not measured, but approximately known (i.e. “open” site)					

Figure 1: Examples of sky view factor (SVF)

a) An example of a SVF of one, for an open site such as a wide field or the top of a large building.



b) In urban areas, the fraction of sky visible from the ground (the SVF) is decreased (less than one) by buildings and vegetation (adapted from Oke 1997; H is the building height; W is the canyon width; UCL is the urban canopy layer)

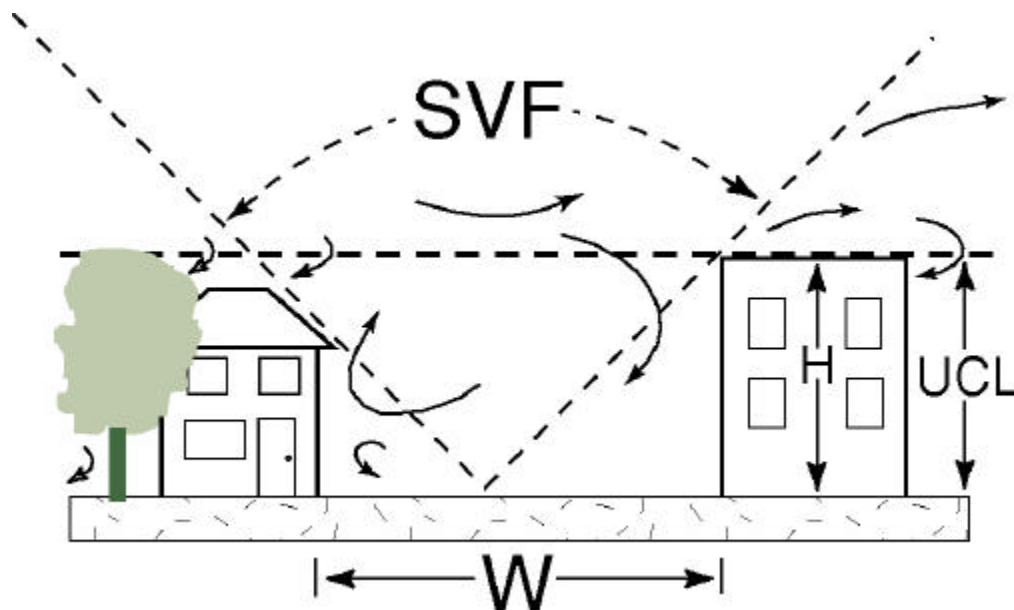


Figure 2: Map of downtown Bloomington, Indiana and a portion of the Indiana University campus showing the relative locations of the observed urban canyons (small rectangles).



Figure 3. Example of a fisheye photo of an urban canyon placed over polar coordinate graph paper used for the manual analysis



Figure 4. Example of the image editing performed prior to digital (automated) analysis of digital fisheye photographs

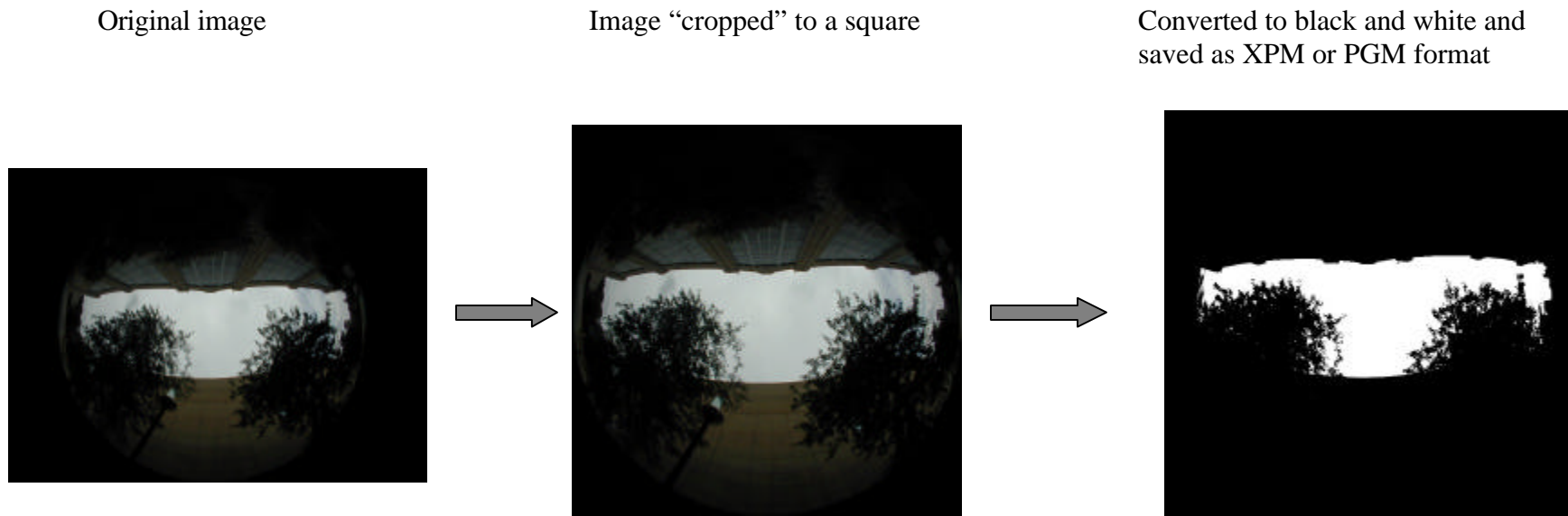


Figure 5: Relative spacing (intervals) at which surface temperature measurements were taken within the canyons

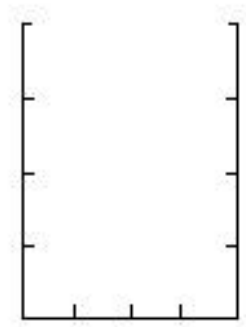


Figure 6: Map showing the mobile transect route taken, and examples of fisheye photographs taken from three portions of the route (A, B, C).

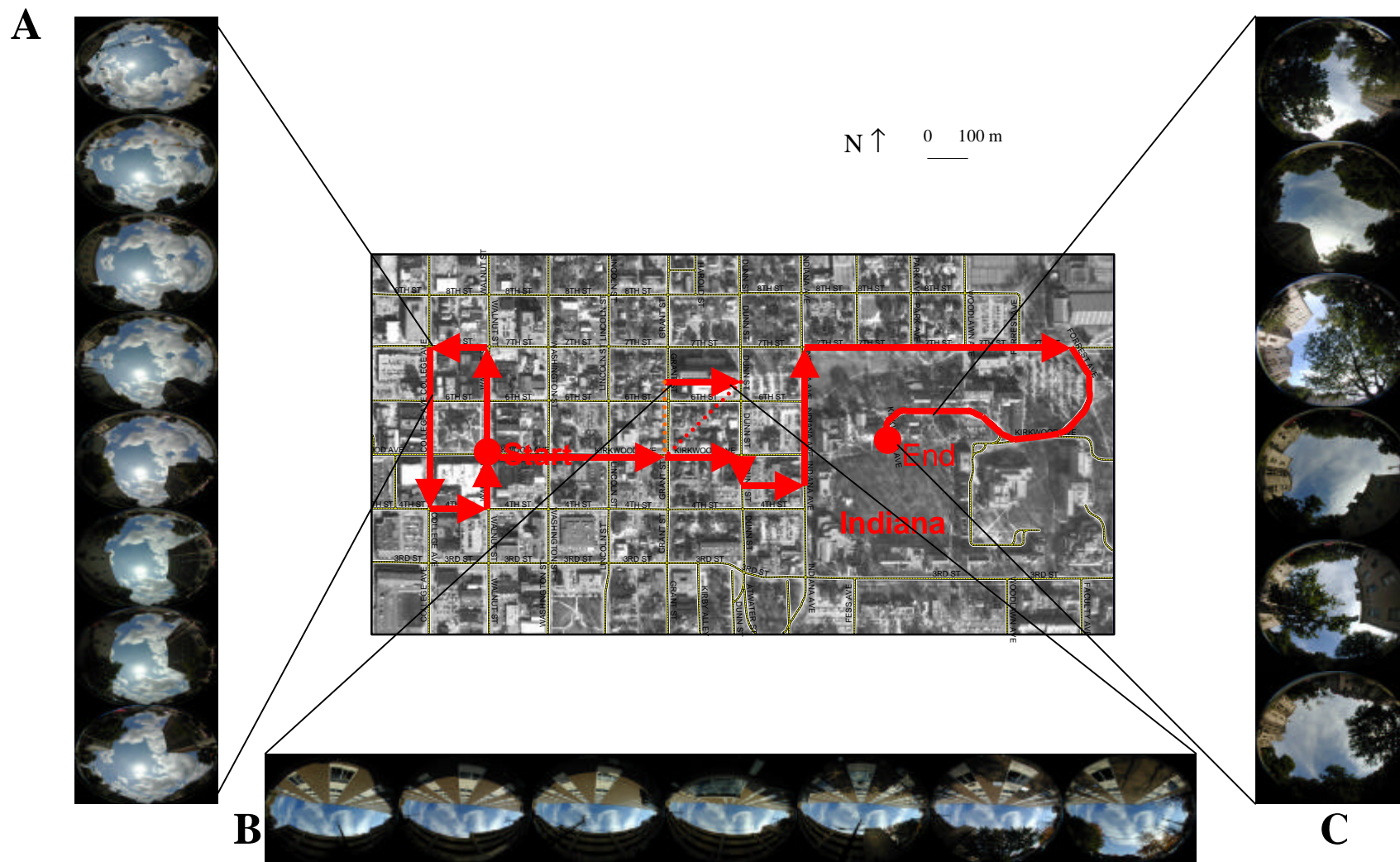


Figure 7. SVF calculated from height and width measurements (H:W), at several different heights (ground, camera height, and LAI height), compared to SVF calculated from the automated analysis of Nikon digital fisheye photographs (camera height).

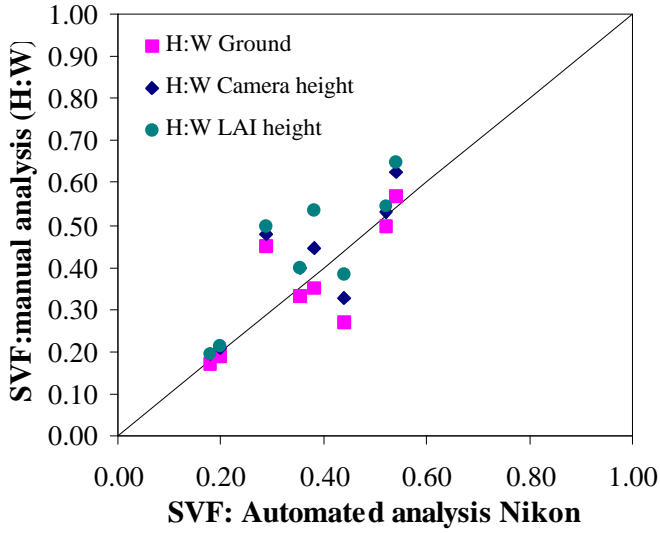


Figure 8. SVF from the manual analysis of fisheye photographs (color and black and white prints from digital Nikon images) using polar coordinate graph paper compared with SVF calculated from the automated analysis of Nikon digital fisheye photographs.

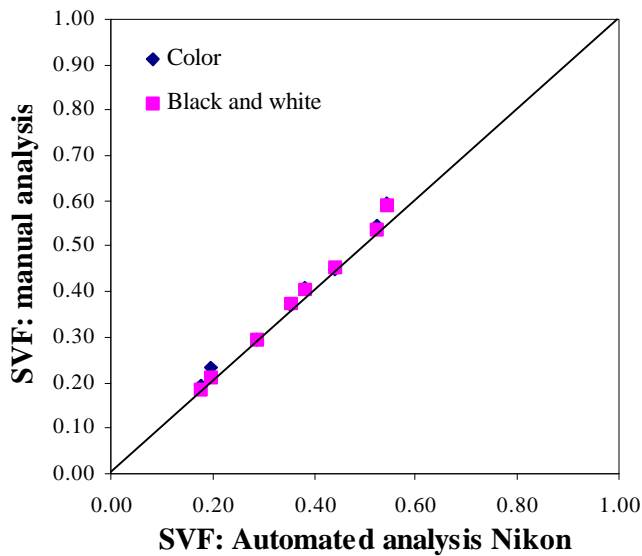


Figure 9. SVF from the manual analysis of fisheye photographs (photograph printout from Sigma lens and manual camera) using polar coordinate graph paper compared with SVF calculated from the automated analysis of Nikon digital fisheye photographs.

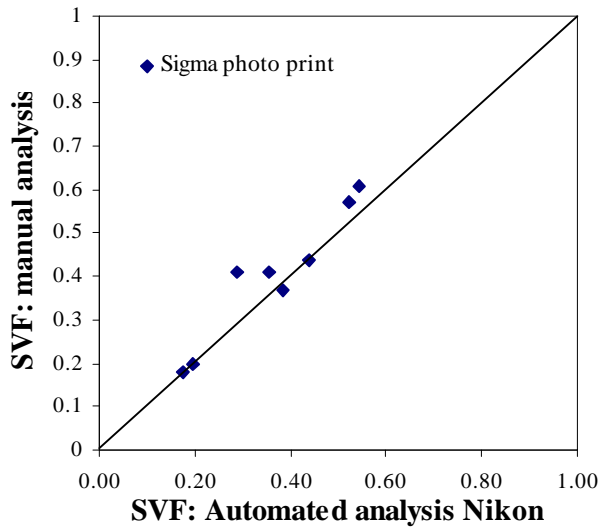


Figure 10. SVF from the automated analysis of LAI 2000 data (DIFN) and from fisheye photographs (scanned into digital format from Sigma lens prints) compared with SVF calculated from the automated analysis of Nikon digital fisheye photographs.

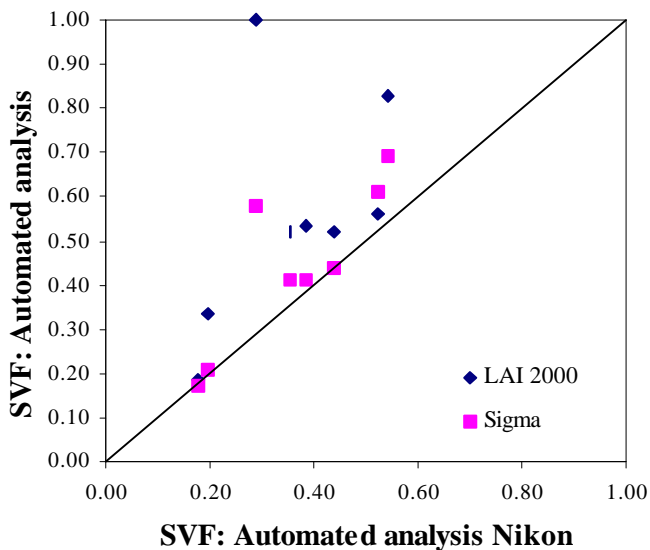


Figure 11. Canyon SVF (automated analysis Nikon) compared with mean surface temperatures (for one day, 4/13/99)

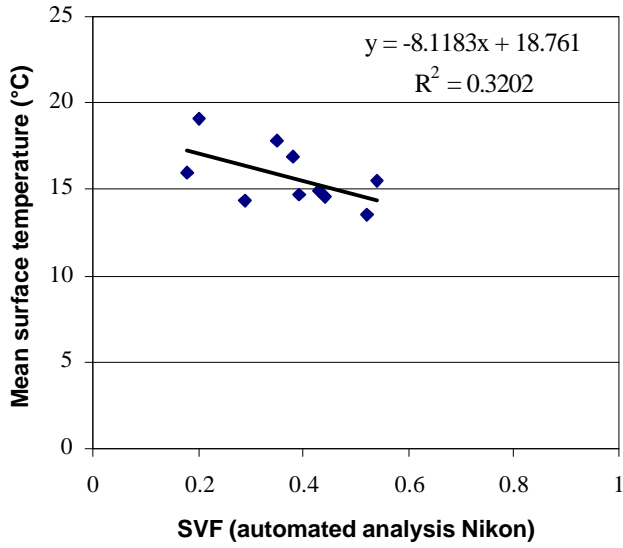


Figure 12. North-South oriented canyon SVF (automated analysis Nikon) compared with mean surface temperatures (for one day, 4/13/99)

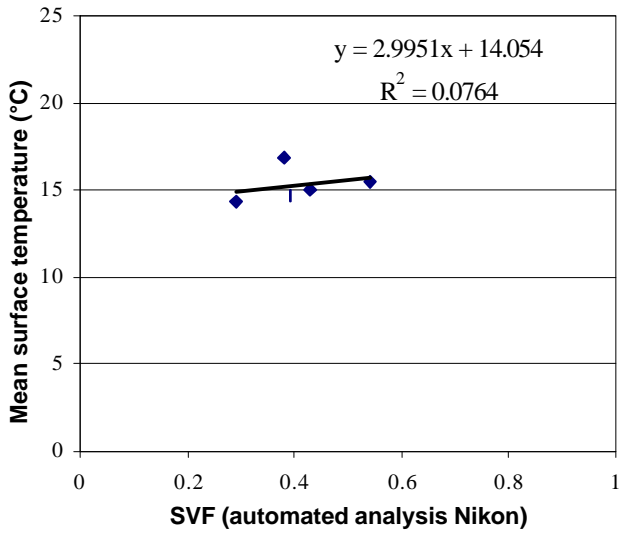


Figure 13. East-West oriented canyon SVF (automated analysis Nikon) compared with mean surface temperatures (for one day, 4/13/99)

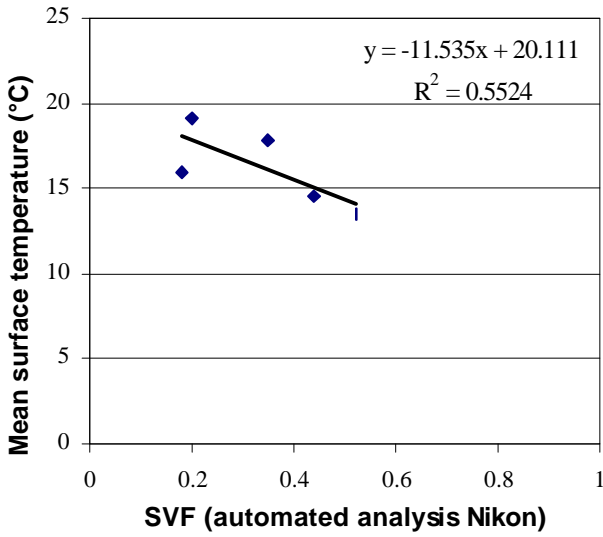


Figure 14. Canyon air temperatures (°C) on day 89 (March 30, 1999), for clear sky conditions

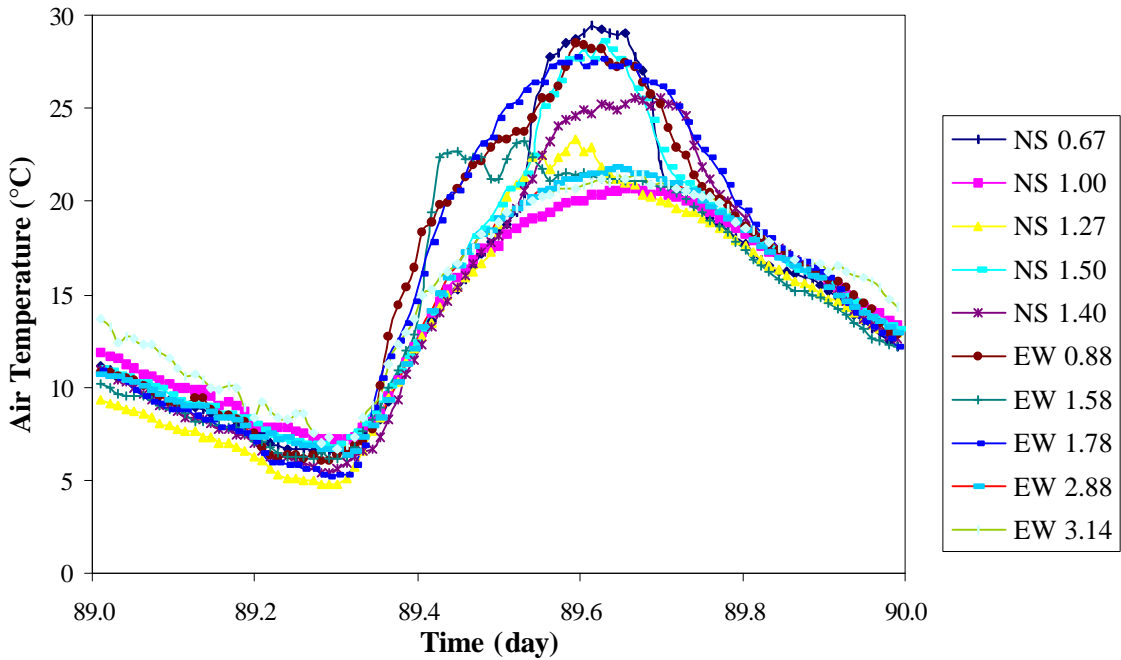


Figure 15. Canyon air temperatures (°C) on day 91 (April 1, 1999), for cloudy (overcast) sky conditions

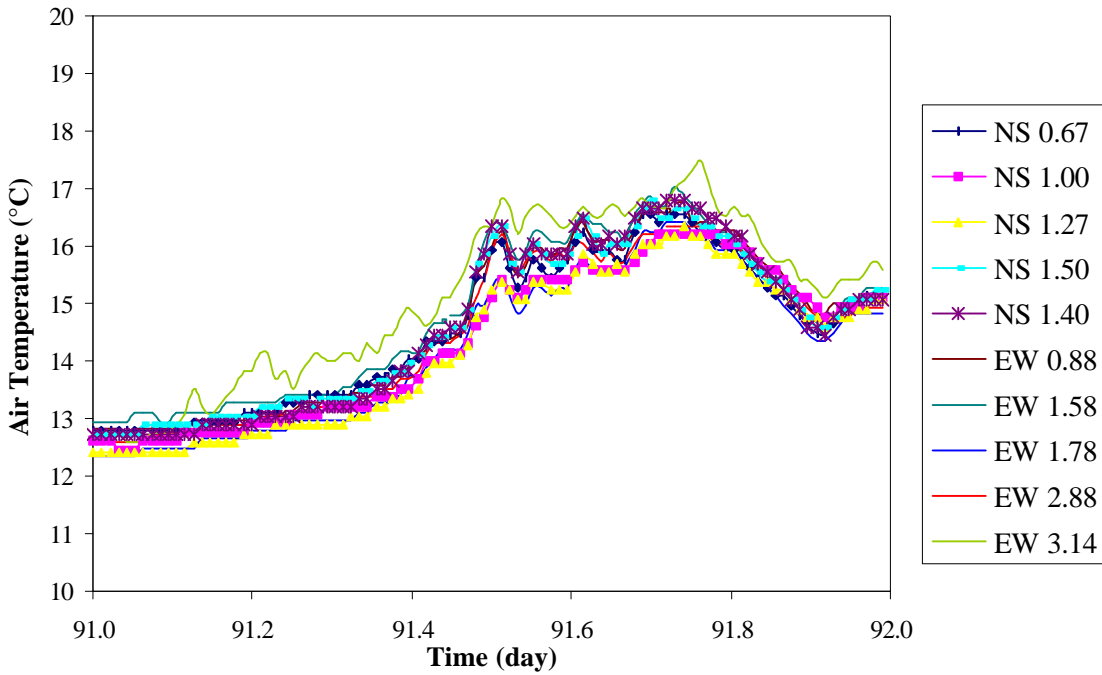


Figure 16. Bloomington weather station air temperature days 89-92 (the first part of day 89 was not available due to absent data).

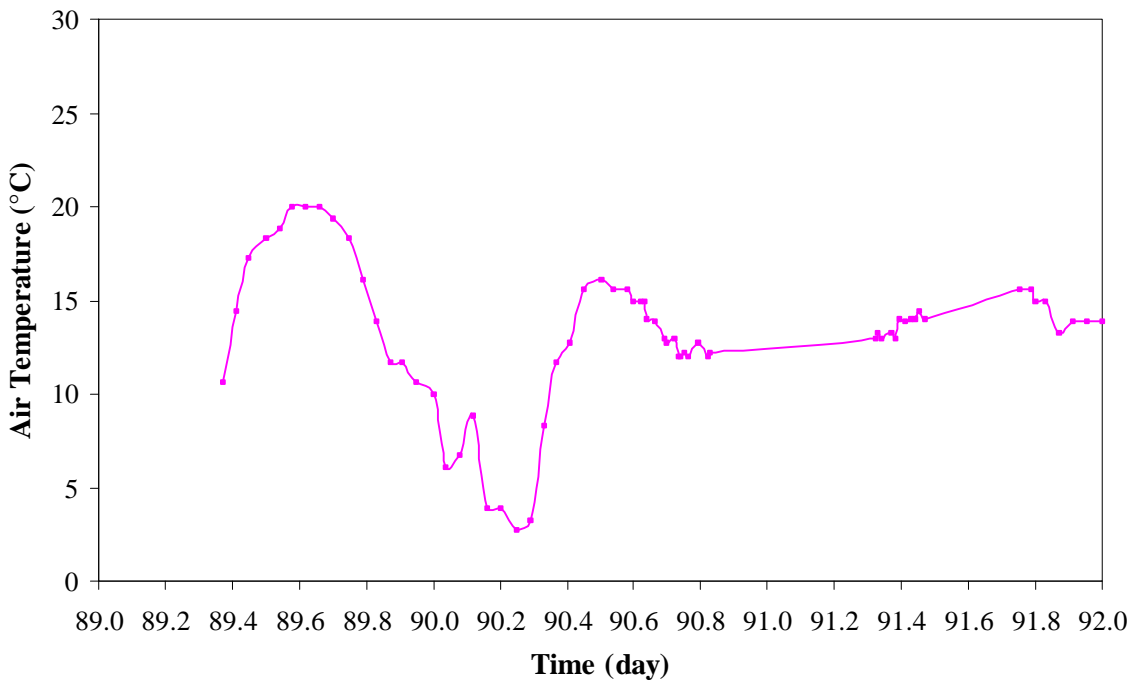


Figure 17. North-South canyon air temperature over a period from clear to cloudy conditions

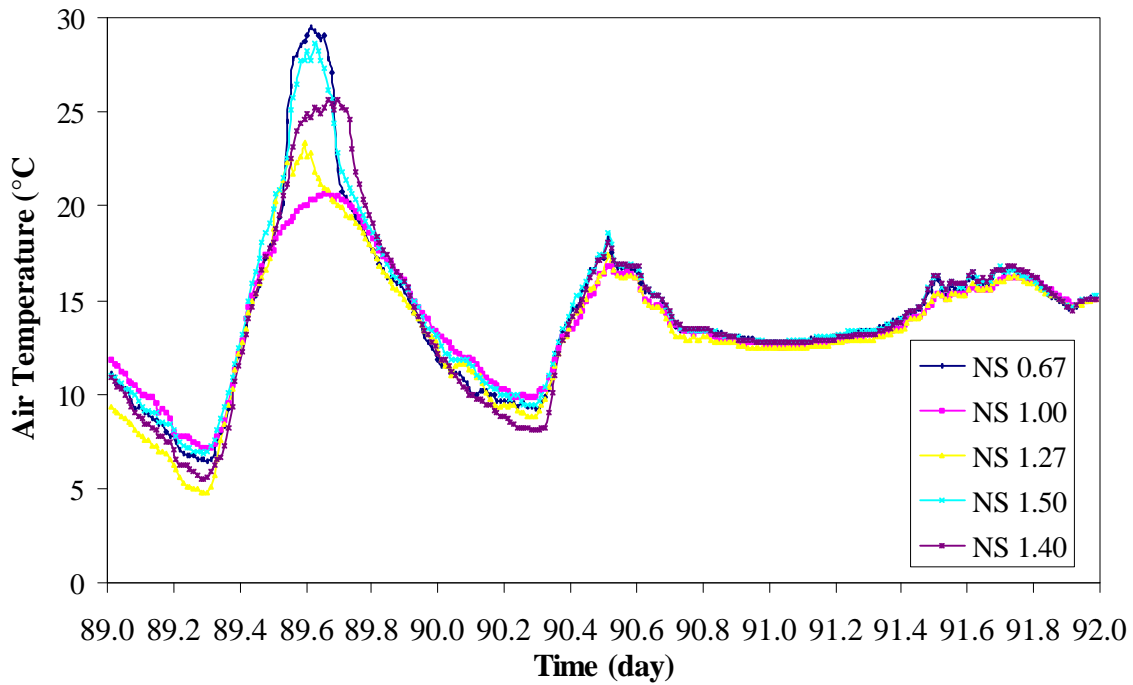


Figure 18. East-West canyon air temperature over a period from clear to cloudy condition

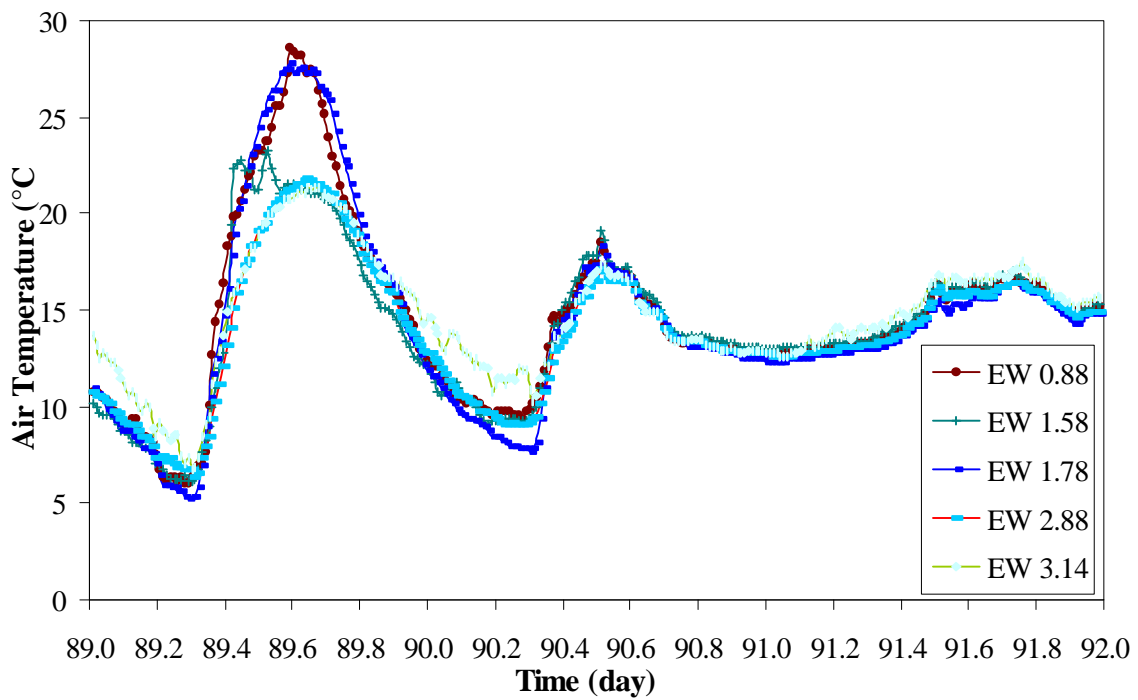


Figure 19. Canyon SVF (automated analysis Nikon) compared with air temperature on 4/13/99

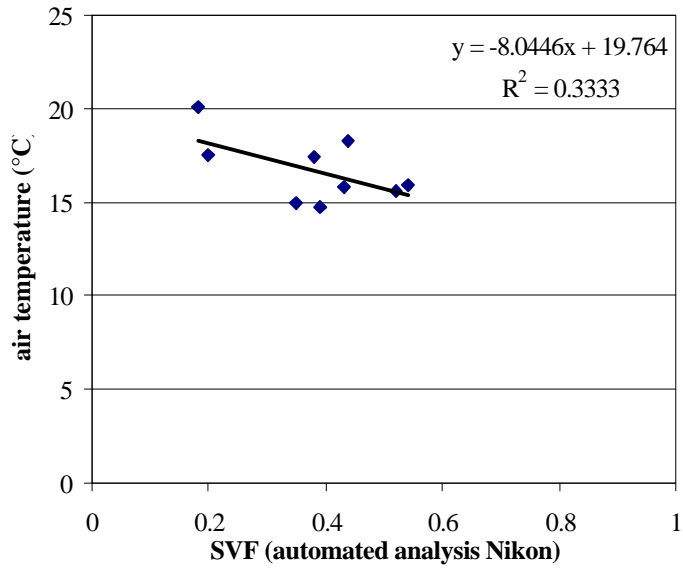


Figure 20. North-South Canyon SVF (automated analysis Nikon) compared with air temperature on 4/13/99

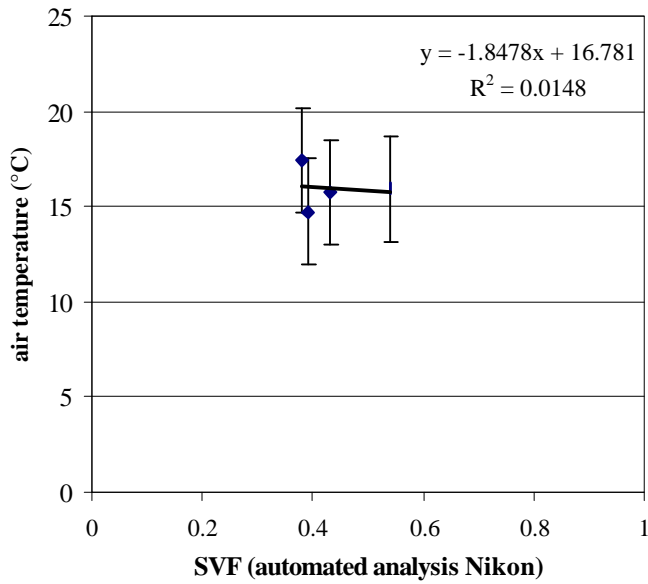


Figure 21. East-West Canyon SVF (automated analysis Nikon) compared with air temperature on 4/13/99

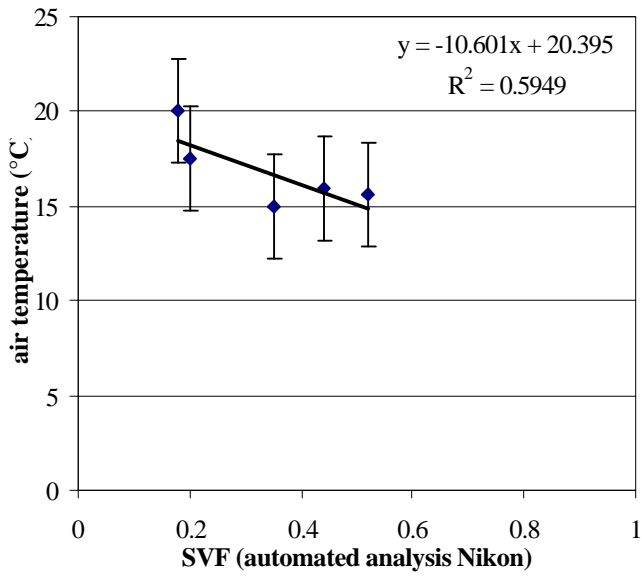


Figure 22. North-South Canyon SVF (H:W) compared with air temperature on 4/13/99

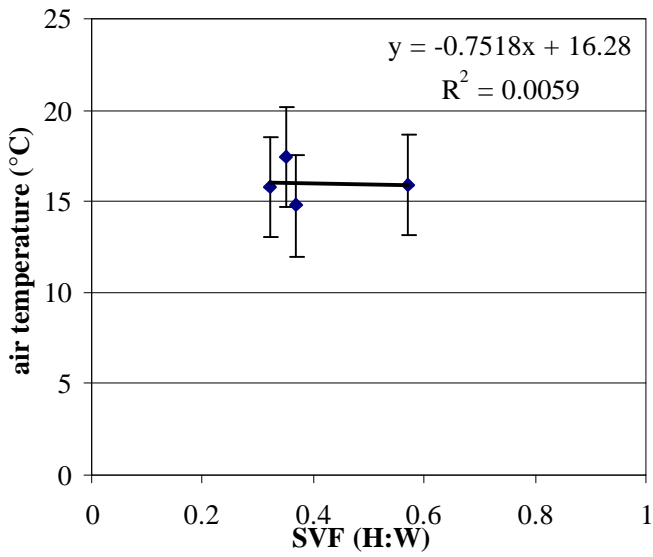


Figure 23. East-West Canyon SVF (H:W) compared with air temperature on 4/13/99

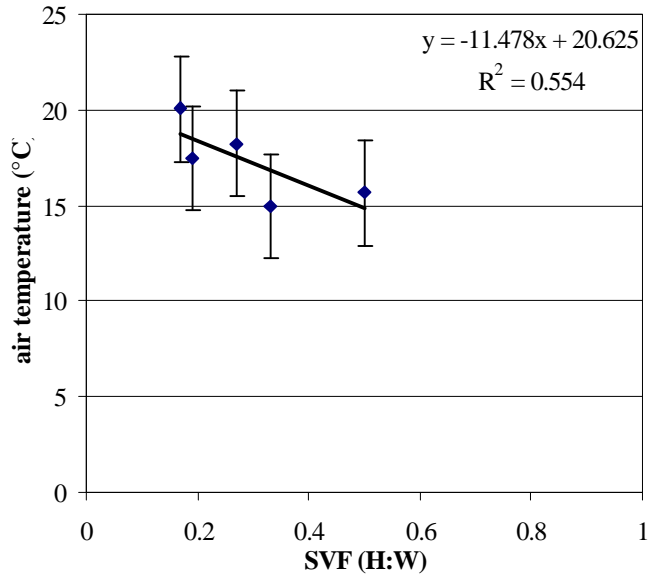
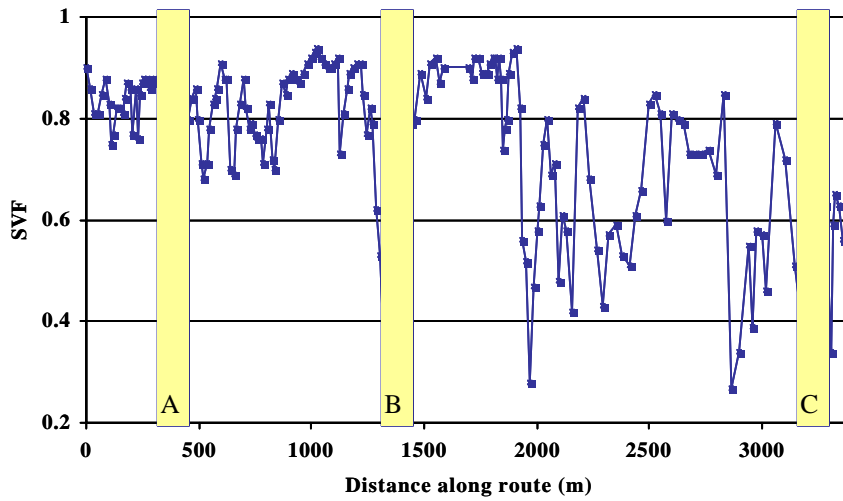


Figure 24. SVF (automated analysis Nikon) variation along the mobile transect. Highlighted portions (A,B,C) correspond to photo segments on Figure 6.



**Appendix 1. Onset HOBO XT temperature loggers accuracy and resolution
(adapted from www.onsetcomp.com, 1999)**

Figure A1: Temperature accuracy of the Onset HOBO loggers. Below, the loggers' **maximum** error is shown. The error assumes all contributing factors to the error are at their maximum values and are aligned so that their values add together. Errors include thermistor error, resistor value errors and quantization error.

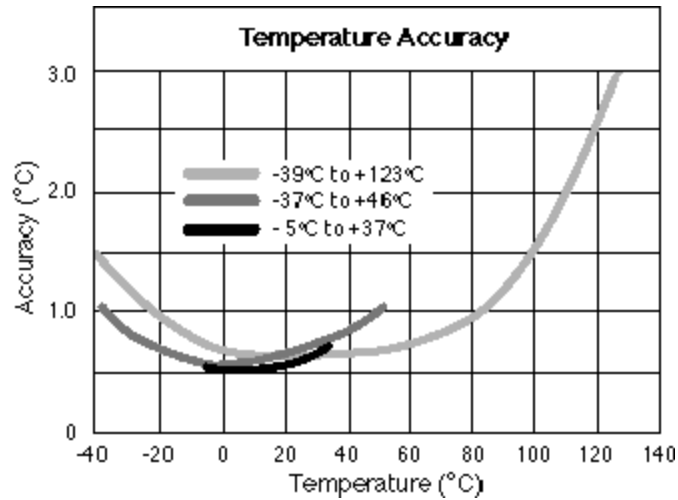


Figure A2: Temperature resolution; the loggers' resolution (difference between temperature steps is shown above).

